The ^{1}H spectrum ($CDCl_3$, room temperature) is rather complex and displays six broad singlets at δ 2.36, 2.21, 2.07, 1.92, 1.59, and 1.55 (of approximately equal intensity) in accord with the six pairs of inequivalent methyl groups that are seen to be present in the molecular structure. The absence of splitting by the ^{31}P nuclei is a phenomenon for which there are several precedents, though no simple explanation. In $Mo_2Cl_4(dmpm)_2$[19] the CH_3 resonances appear as singlets, and a similar observation has been made for $Mn_2(CO)_6(dmpm)_2$.[20] Other examples of small or nondetectable ^{31}P–^{1}H coupling of this sort will be found in other reports.[21,22] The methylene ^{1}H resonances are seen as an AB pattern centered at δ 4.40 (J_{AB} = 13.4 Hz) and a broad peak at δ 3.95, in an intensity ratio of 2:1. The absence of an AB pattern in the second resonance may be due to a slow motion of the unique methylene group from side to side. Unfortunately, the solubility of this compound is too low to permit low-temperature NMR studies.

Acknowledgments. We thank the National Science Foundation for the support of this research through grants to R.A.W. (Grant No. CHE85-06702) and F.A.C. (Grant No. CHE82-11407).

Registry No. $Re_2Cl_4(\mu\text{-dmpm})_3$, 103852-11-5; $(n\text{-}Bu_4N)_2Re_2Cl_8$, 14023-10-0; $Re_2Cl_4(P\text{-}n\text{-}Pr_3)_4$, 52359-07-6.

Supplementary Material Available: Tables of torsion angles and anisotropic displacement parameters for both structures and figures showing contoured Fourier sections from both structures (10 pages); tables of observed and calculated structure factors for both structures (35 pages). Ordering information is given on any current masthead page.

---

(19) Cotton, F. A.; Walton, R. A., unpublished work.

(20) Lemke, F. R.; Kubiak, C. P. *Inorg. Chim. Acta* **1986**, *113*, 125.

(21) King, R. B.; Raghuveer, K. S. *Inorg. Chem.* **1984**, *23*, 2482.

(22) Wong, W. K.; Chiu, K. W.; Wilkinson, G.; Howes, A. J.; Motevalli, M.; Hursthouse, M. B. *Polyhedron* **1985**, *4*, 603.

Contribution from the Department of Chemistry and Laboratory for Molecular Structure and Bonding,
Texas A&M University, College Station, Texas 77843

Quadruply Bonded $Mo_2I_4(dppe)_2$ (dppe = Bis(diphenylphosphino)ethane): Twisted and Eclipsed Rotational Conformations and Their Significance

F. Albert Cotton,* Kim R. Dunbar, and Marek Matusz

Received April 22, 1986

The structural characterizations of two crystallographic forms of β-$Mo_2I_4(dppe)_2$ are reported, and the relationship between the degree of torsional twist that the molecules exhibit in the solid state and the energy of the $\delta \rightarrow \delta^*$ transition is discussed. The title compound can be prepared by reaction of the quadruply bonded $Mo_2(\mu\text{-}O_2CCH_3)_4$ with Me_3SiI in toluene in the presence of 2 equiv of dppe and can be crystallized from many solvents. A solution of the compound in dichloromethane–methanol produces green monoclinic crystals of the dichloromethane solvate β-$Mo_2I_4(dppe)_2\cdot{}^2/_3CH_2Cl_2$ (**1**), in which there are twisted molecules, **1a**, located on a general position, and eclipsed molecules, **1b**, which reside on crystallographic inversion centers. The crystal belongs to the space group $P2_1/n$ with unit cell dimensions a = 13.600 (4) Å, b = 17.755 (5) Å, c = 30.30 (1) Å, β = 98.74 (2)°, V = 8426 (4) Å^3, and Z = 6. The asymmetric unit is defined by 1.5 molecular formulas of $Mo_2I_4(dppe)_2$ and one CH_2Cl_2 molecule. The structure is unusual in that **1a** possesses a mean torsional twist angle of χ = 27.9° and **1b** assumes the fully eclipsed orientation with an average χ = 0°, where χ is the angle of internal rotation away from the eclipsed conformation. A significant difference exists in the degree of Mo–Mo interaction for **1a** and **1b** as is evident from the Mo–Mo bond distances of 2.180 (4) and 2.129 (5) Å for the cocrystallized molecules **1a** and **1b**, respectively. A second crystal of $Mo_2I_4(dppe)_2$ was grown from a dichloromethane–toluene mixture and is designated as β'-$Mo_2I_4(dppe)_2\cdot C_7H_8$ (**2**). The β' form crystallizes in the monoclinic $P2_1/n$ space group with the following unit cell dimensions: a = 12.015 (2) Å, b = 25.048 (4) Å, c = 19.407 (4) Å, β = 95.3 (2)°, V = 5814 (2) Å^3, and Z = 4. The midpoints of the Mo–Mo bonds reside on a set of general positions. The molecule is internally rotated by an average value of χ = 25.7°, and the Mo–Mo distance is 2.179 (3) Å. The variation in δ overlap in the three different types of molecules **1a**, **1b**, and **2** was effectively probed by recording the visible spectra of the samples in the solid state. Two distinct bands are observed at 670 nm (14 900 cm^{-1}) and at 920 nm (10 900 cm^{-1}) in the spectrum of β-$Mo_2I_4(dppe)_2\cdot{}^2/_3CH_2Cl_2$ and are assigned to the $\delta \rightarrow \delta^*$ ($A_{1g} \rightarrow A_{1u}$) transitions of molecules **1b** (χ = 0°) and **1a** (χ = 27.9°), respectively; the intensity ratio is in approximate accord with the ratio of the δ/δ overlap integrals. The solid-state visible spectrum of β'-$Mo_2I_4(dppe)_2\cdot C_7H_8$ contains only one band at λ_{max} = 878 nm (11 400 cm^{-1}), in agreement with the results of the X-ray structure, which shows that only one type of molecule is present. Dichloromethane solution spectra of both β and β' forms are identical, with the $\delta \rightarrow \delta^*$ transition being located at 860 nm (11 600 cm^{-1}). The electronic absorption properties of **1** and **2** as well as the results of $^{31}P\{^1H\}$ NMR spectroscopy and cyclic voltammetry studies are discussed.

Introduction

Compounds of the type $Mo_2X_4(LL)_2$, where X = Cl or Br and LL is a bridging bidentate phosphine $R_2P(CH_2)_nPR_2$, have been interesting subjects for structural and spectroscopic studies.[1-7] X-ray crystallographic data for those with n = 1, i.e., the bis(diphenylphosphino)methane complexes, $Mo_2X_4(dppm)_2$ (X = Cl[8], Br[4], I[9]), have shown that the ligands adopt a fully eclipsed orientation across the two metal centers, with the dppm ligands in a trans bridging disposition. In the case of n = 2, as in $Mo_2X_4(dmpe)_2$ or $Mo_2X_4(dppe)_2$ (X = Cl, Br; dmpe = bis(dimethylphosphino)ethane, dppe = bis(diphenylphosphino)ethane), the molecules exhibit various degrees of torsional twist about the Mo–Mo axis, resulting from the conformational preference of the fused, six-membered rings that are present in these β-$Mo_2X_4(LL)_2$ molecules.

It can be shown from the angular parts of the orbital wave functions that the strength of the δ component of a quadruple bond should vary with cos (2χ), where χ is the angle of internal rotation away from the eclipsed conformation (χ = 0°).[10] Extensive studies conducted in this group, based upon data from 10 related, structurally characterized compounds, have shown that the Mo–Mo distance in the $Mo_2X_4(LL)_2$ class of molecules varies linearly with cos (2χ).[4,7] An analysis of the variation in $\delta \rightarrow \delta^*$ transition energy with δ-bond strength (measured by Mo–Mo bond length)

---

(1) Cotton, F. A.; Powell, G. L. *Inorg. Chem.* **1983**, *22*, 1507.

(2) Agaskar, P. A.; Cotton, F. A.; Fraser, I. F.; Peacock, R. D. *J. Am. Chem. Soc.* **1984**, *106*, 1851.

(3) Agaskar, P. A.; Cotton, F. A. *Inorg. Chem.* **1984**, *23*, 3383.

(4) Campbell, F. L., III.; Cotton, F. A.; Powell, G. L. *Inorg. Chem.* **1984**, *23*, 4222.

(5) Campbell, F. L., III.; Cotton, F. A.; Powell, G. L. *Inorg. Chem.* **1985**, *24*, 177.

(6) Agaskar, P. A.; Cotton, F. A.; Derringer, D. R.; Powell, G. L.; Root, D. R.; Smith, T. J. *Inorg. Chem.* **1985**, *24*, 2786.

(7) Campbell, F. L., III.; Cotton, F. A.; Powell, G. L. *Inorg. Chem.* **1985**, *24*, 4384.

(8) Abbott, E. H.; Bose, K. S.; Cotton, F. A.; Hall, W. T.; Sekutowski, J. C. *Inorg. Chem.* **1978**, *17*, 3240.

(9) Cotton, F. A.; Dunbar, K. R.; Poli, R. *Inorg. Chem.*, in press.

(10) Cotton, F. A.; Fanwick, P. E.; Fitch, J. W.; Glicksman, H. D.; Walton, R. A. *J. Am. Chem. Soc.* **1979**, *101*, 1752.

0020-1669/86/1325-3641$01.50/0

Table I. Summary of Crystal Data, Data Collection Parameters, and Least-Squares Residuals for β-$Mo_2I_4(dppe)_2 \cdot {}^2/_3CH_2Cl_2$ (**1**) and β'-$Mo_2I_4(dppe)_2 \cdot C_7H_8$ (**2**)

	1	**2**
formula	$Mo_2I_4P_4C_{52}H_{48} \cdot 0.66CH_2Cl_2$	$Mo_2I_4P_4C_{52}H_{48} \cdot C_7H_8$
fw	1552.87	1588.50
space group	$P2_1/n$	$P2_1/n$
syst abs	$h0l$ $(h + l = 2n)$, $0k0$ $(k = 2n)$	$h0l$ $(h + l = 2n)$, $0k0$ $(k = 2n)$
a, Å	13.600 (4)	12.015 (2)
b, Å	17.755 (5)	25.048 (4)
c, Å	35.30 (1)	19.407 (4)
α, deg	90.0	90.0
β, deg	98.74 (2)	95.51 (2)
γ, deg	90.0	90.0
V, Å^3	8426 (4)	5814 (2)
Z	6	4
d_{calcd}, g/cm^3	1.836	1.815
cryst size, mm	0.10 × 0.32 × 0.40	0.10 × 0.12 × 0.30
μ(Mo Kα), cm^{-1}	28.21	26.68
data colln instrum	Nicolet P3	Nicolet P3
radiation (monochromated in incident beam)	d	d
orientation reflcns: no.; range (2θ), deg	25; $20 < 2\theta < 25$	25; $20 < 2\theta < 25$
temp, °C	22 ± 1	22 ± 1
scan method	ω-scan	ω-scan
data colln range (2θ), deg	$4 < 2\theta < 45$	$4 < 2\theta < 45$
no. of unique data, total with $F_o^2 > 3\sigma(F_o^2)$	7631, 4098	4026, 2499
no. of params refined	459	331
transmissn factors: max, min	90.10, 69.80	99.17, 84.73
R^a	0.0677	0.0635
$R_w{}^b$	0.0827	0.0791
quality-of-fit indicator^c	1.227	1.274
largest shift/esd, final cycle	0.11	0.18
largest peak, e/Å^3	2.25	0.95

$^a R = \sum||F_o| - |F_c||/\sum|F_o|$. $^b R_w = [\sum w(|F_o| - |F_c|)^2/\sum w|F_o|^2]^{1/2}$; $w = 1/\sigma^2(|F_o|)$. ^{c}Quality of fit $= [\sum w(|F_o| - |F_c|)^2/(N_{observns} - N_{params})]^{1/2}$. ^{d}Mo K$\alpha$ ($\lambda\bar{\alpha}$ = 0.71073 A); graphite monochromated.

for the same group of 10 complexes revealed a nonlinear dependence, a result that is in excellent accord with theoretical considerations.[5]

The present work is an interesting extension of the earlier studies. We now report structural and visible spectroscopic data for three molecules of the $Mo_2X_4(LL)_2$ type, which contain *identical* ligand sets yet exhibit different rotational conformations. The quadruply bonded β-$Mo_2I_4(dppe)_2$ species crystallizes as the dichloromethane solvate β-$Mo_2I_4(dppe)_2 \cdot {}^2/_3CH_2Cl_2$ (**1**) and as the toluene solvate β'-$Mo_2I_4(dppe)_2 \cdot C_7H_8$ (**2**). The crystal structure of **1** consists of two independent dimolybdenum molecules (**1a** and **1b**) possessing different angles of internal rotation, and the X-ray data for **2** reveal a third rotational conformation. These results provide for the first time a correlation of both Mo–Mo bond distance and $\delta \rightarrow \delta^*$ transition energy with twist angle without any change in the identity of either X or LL in an $Mo_2X_4(LL)_2$ type compound.

Experimental Section

Unless otherwise stated, all manipulations were performed under anaerobic conditions with standard vacuum line and Schlenk techniques. The solvents were freshly distilled prior to use. Bis(diphenylphosphino)ethane (dppe) was purchased from Strem Chemicals Inc. and was used without further purification. The iodotrimethylsilane reagent (Me_3SiI) was obtained from Aldrich Chemical Co. $Mo_2(O_2CCH_3)_4$ was prepared according to published procedures.[11]

A. Preparations. (i) β-$Mo_2I_4(dppe)_2 \cdot {}^2/_3CH_2Cl_2$. A mixture comprising $Mo_2(O_2CCH_3)_4$ (0.50 g, 1.17 mmol), dppe (0.93 g, 2.34 mmol), and Me_3SiI (0.665 mL, 4.70 mmol) in toluene (50 mL) was refluxed for 0.5 h. During this time the pale yellow solution containing a suspension of $Mo_2(O_2CCH_3)_4$ turned red-brown, and precipitation of a brown solid occurred. The solution was stirred for an additional 5 h at room temperature after which time the volume was reduced to 30 mL. The reaction mixture was filtered, and the crude brown product was washed with toluene followed by diethyl ether and recrystallized by slow addition of MeOH to a chilled, concentrated CH_2Cl_2 solution. The resulting green microcrystalline material was dried in vacuo for 3 h to give a yellow-gold powder, yield 1.56 g (89%). Anal. Calcd for $C_{52}H_{48}I_4P_4Mo_2$: C, 41.97; H, 3.25; I, 34.10. Found: C, 41.49; H, 3.43; I, 33.88. Large green plate-like crystals of β-$Mo_2I_4(dppe)_2 \cdot {}^2/_3CH_2Cl_2$ were grown by carefully layering MeOH over a concentrated solution of the gold powder in CH_2Cl_2. The crystals deposited on the bottom of the flask after the solution sat undisturbed for several days at room temperature.

(ii) β'-$Mo_2I_4(dppe)_2 \cdot C_7H_8$. The synthetic details for the bulk preparation of β-$Mo_2I_4(dppe)_2$ as a gold powder are described above in part A(i). Crystals of the amber β' form of $Mo_2I_4(dppe)_2$ were grown by slow evaporation of a red-brown solution of the gold powder dissolved in dichloromethane–toluene (4:1). Small, dark amber rods formed after 1 week in air.

B. X-ray Structure Analysis. (i) Data Collection and Reduction. A thin green crystal of **1** with approximate dimensions 0.10 × 0.32 × 0.40 mm and a red-brown crystal of **2** measuring 0.10 × 0.12 × 0.30 mm were each mounted on the tip of a glass fiber and coated with epoxy resin. Geometric and intensity data for **1** and **2** were collected at room temperature on an automated Nicolet P3 four-circle diffractometer equipped with Mo Kα radiation. The procedures employed for data collection have been described previously.[12] Both crystals were found to be monoclinic, and in each case the unit cell parameters and orientation matrix were refined by a least-squares fit to the positions of 25 reflections in the range $20 < 2\theta < 30°$. The lattice dimensions and the presence of a mirror plane were verified by axial photography. The ω-scan technique was used to scan data points in the range $4 \leq 2\theta \leq 45°$. In both cases, three check reflections monitored throughout data collection displayed no significant gain or loss in intensity. Data reduction was carried out by standard methods using well-established computational procedures.[13a] The data were corrected for Lorentz and polarization effects, and azimuthal scans (ψ-scans) of nine reflections having an Eulerian angle χ near 90° were used as a basis for an empirical absorption correction for **1**.[13b] Pertinent crystallographic parameters for **1** and **2** are summarized in Table I.

(ii) Structure Solution and Refinement. β-$Mo_2I_4(dppe)_2 \cdot {}^2/_3CH_2Cl_2$ (1). Axial photographs and systematic absences from the data indicated that the crystal is monoclinic and belongs to the space group $P2_1/n$. The positions of the three unique Mo atoms were determined by application of direct methods (Multan 11/82). Two of the Mo atoms define a

---

(11) Brignole, A. B.; Cotton, F. A. *Inorg. Synth.* **1972**, *13*, 81.

(12) Cotton, F. A.; Frenz, B. A.; Deganello, G.; Shaver, A. *J. Organomet. Chem.* **1973**, *50*, 227.

(13) (a) Data processing was done on a PDP-11/60 computer with PDP-11 simulated VAXSDP and on a VAX-11/780 computer with programs from the package VAXSDP. (b) North, A. C. T.; Phillips, D. C.; Mathews, F. S. *Acta Crystallogr., Sect. A: Cryst. Phys., Diffr., Theor. Gen. Crystallogr.* **1968**, *A24*, 351.

molecule of $Mo_2I_4(dppe)_2$ that resides on a general position (**1a**), and a third Mo is associated with another dimeric unit (**1b**), the midpoint of which lies on a crystallographic inversion center. A series of alternating least-squares refinements and difference Fourier maps led to complete development of the coordination spheres of the two independent molecules. In the later stages of the refinement, two distinct areas of electron density in the Fourier maps remained unaccounted for. These peaks are not in close proximity to the atoms of the dimolybdenum molecule and were assumed to be part of lattice solvent molecules. One set of these peaks was successfully modeled as a CH_2Cl_2 molecule on a general position, but another lone peak of 2.25 e/Å^3 did not refine well and after several attempts to model it, we excluded it from the calculations. In the final refinement 4098 data were used to fit 459 variable parameters (data:parameter ratio 9:1), giving convergence with residuals of R = 0.0677 and R_w = 0.0827 and a quality of fit index equal to 1.22. The final least-squares cycle did not shift any parameter by more than 0.11 times its estimated standard deviation. Table II contains the positional and thermal parameters for **1**. Selected bond distances and angles are summarized in Table III.

β'-$Mo_2I_4(dppe)_2\cdot C_7H_8$ (2). The structure of **2** was refined in the monoclinic space group $P2_1/n$, uniquely determined by the systematic absences from the data. The positions of the two Mo atoms were determined by direct-methods procedures, and all other atoms were located in difference Fourier maps. The molecule does not possess any crystallographic symmetry, and the unit cell consists of four molecules of $Mo_2I_4(dppe)_2$ and four toluene solvent molecules, each set located on a fourfold general equipoint. The toluene molecule showed rotational disorder (around the sixfold axis of the phenyl ring). Two major orientations were located, and each methyl carbon was assigned half-occupancy. A total of 70 non-hydrogen atoms were located, but only the heavy atoms Mo, I, and P were refined anisotropically. Convergence was reached using 2499 data with $F^2_{obsd} > 3\sigma(F_{obsd})^2$ to fit 331 variables for a data to parameter ratio of 7.5. The largest shift/esd in the final least squares cycle was 0.18 and the highest peak in the last difference Fourier map was 0.95 e/Å^3. The refinement gave residuals (defined in Table I) of R = 0.0635 and R_w = 0.0791 and quality of fit index of 1.271.

Physical Measurements. Electronic spectra were measured on dichloromethane solutions or on Nujol mulls with a Cary 17D spectrophotometer. Electrochemical measurements were performed with a Bioanalytical Systems, Inc., Model BAS 100 electrochemical analyzer in conjunction with a Bausch and Lomb, Houston Instruments Model DMP 40 digital plotter. Experiments were carried out in dichloromethane containing 0.2 M tetra-*n*-butylammonium hexafluorophosphate (TBAH) as a supporting electrolyte. A three-electrode cell configuration was used, with a platinum disk, Model BAS MF 2032, and a platinum wire as working and auxiliary electrodes respectively. A BAS MF 2020 Ag/AgCl cell was used as a reference electrode (against which ferrocene is oxidized at $E_{1/2}$ = +0.52 V). All potentials were referenced to the Ag/AgCl electrode at 22 ± 2 °C with a full positive feedback resistance compensation and are uncorrected for junction potentials. $E_{1/2}$ values were determined as $(E_{p,a} + E_{p,c})/2$. $^{31}P\{^1H\}$ NMR spectra were recorded on a Varian XL-200 spectrometer operated at 80.98 MHz. ^{31}P resonances were referenced to an external standard of aqueous 85% H_3PO_4. Microanalyses were performed by Galbraith Laboratories of Knoxville, TN.

Results and Discussion

Preparation and Preliminary Characterization of β-Mo_2I_4(dppe)$_2$. A. Synthetic Methods. Few iodo compounds of multiply bonded transition metals have been reported. Until recently the only documented examples were complexes of the type $Re_2I_4L_4$ and $Re_2I_4(LL)_2$ (L = PEt_3, P-*n*-Pr_3, P-*n*-Bu_3, LL = dppe, arphos)[14] prepared from $Re_2I_8^{2-}$ and the quadruply bonded $Mo_2I_4(P\text{-}n\text{-}Pr_3)_4$[15] and $Mo_2I_4(bpy)_2$.[16] One additional compound, tentatively formulated as $Mo_4I_6(dppe)_2$, was reported by Walton et al.,[14] from the reaction of $Mo_4I_{11}^{2-}$ with dppe. A comparison of our present results with the physical and spectroscopic properties reported by Walton clearly indicates that the dppe species in ref 14 is not β-$Mo_2I_4(dppe)_2$.

Recently we have been preparing dimolybdenum(II) complexes from reactions of Me_3SiX (X = Cl, Br, I) with $Mo_2(\mu\text{-}O_2CCH_3)_4$.[2-5,17] This method had earlier proved to be convenient for preparing chloro and bromo complexes, and an extension of this chemistry to include the iodo compounds $Mo_2I_4(dppm)_2$[18] and $Mo_2I_4(dppe)_2$ has been accomplished. The reaction proceeds in THF or toluene to afford virtually quantitative yields of the bridging (β) form of $Mo_2X_4(LL)_2$. The chelating forms (α) of $Mo_2X_4(dppe)_2$ (X = Cl, Br) can be isolated from the same reaction mixture when mild conditions are employed. Investigations into the preparation of these isomers have revealed that the α form is the kinetic product and it rearranges to the thermodynamically favored β form in solution and in the solid state. The mechanism of the isomerization has been the subject of several studies, and the results support a unimolecular process.[2,6,19]

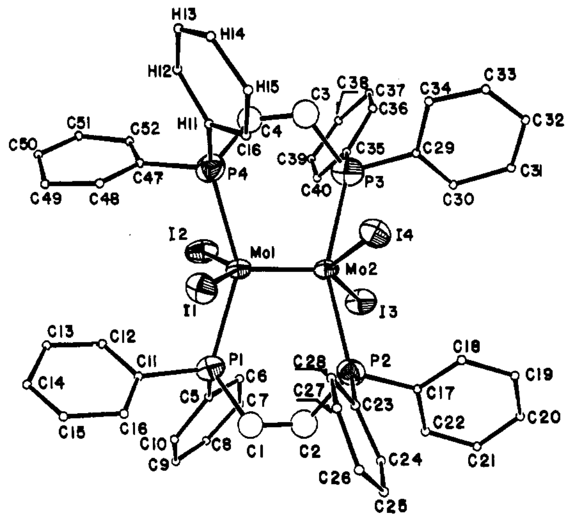

Figure 1. ORTEP view of molecule **1a** in β-$Mo_2I_4(dppe)_2\cdot{}^2/_3CH_2Cl_2$ (**1**) Phenyl-group carbon atoms are shown as small circles for clarity. All other atoms are represented by their 50% probability ellipsoids.

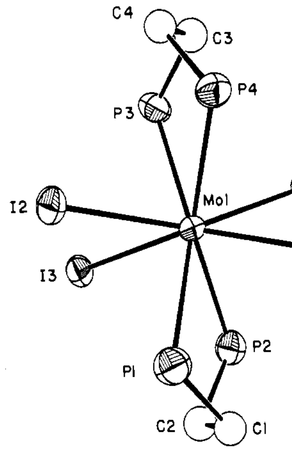

Figure 2. Central portion of β-$Mo_2I_4(dppe)_2$ (**1a**) viewed along the Mo(1)-Mo(2) axis.

In the present case, in view of the forcing thermal conditions that were used, the α form was not isolated although presumably it could be prepared by suitably adjusting the experimental conditions. The β form precipitates from toluene after a short reflux period, and recrystallization of the crude product leads to a microcrystalline green compound that rapidly loses solvent upon vacuum-drying. The resulting gold powder is analytically pure and was used to prepare suitable single crystals of **1** and **2**.

B. Structural Results. Two different crystalline substances were obtained depending on the crystallization solvent used; the structures of both have been solved and refined. Form **1** presents us with the remarkable situation in which two quite different rotomers are present in the same unit cell; one type of molecule (**1a**) occupies the fourfold general position and has a twisted rotational conformation (χ = 27.9°), while the other type (**1b**)

---

(14) Glicksman, H. D.; Walton, R. A. *Inorg. Chem.* **1978**, *17*, 3197.

(15) Glicksman, H. D.; Walton, R. A. *Inorg. Chem.* **1978**, *17*, 200.

(16) Brencic, J. V.; Dobcnik, D.; Segedin, P. *Monatsh. Chem.* **1976**, *107*, 395.

(17) Agaskar, P. A.; Cotton, F. A. *Rev. Chim. Miner.* **1985**, *22*, 302.

(18) Cotton, F. A.; Dunbar, K. R.; Poli, R. *Inorg. Chem.*, in press.

(19) Agaskar, P. A.; Cotton, F. A. *Inorg. Chem.* **1986**, *25*, 1.

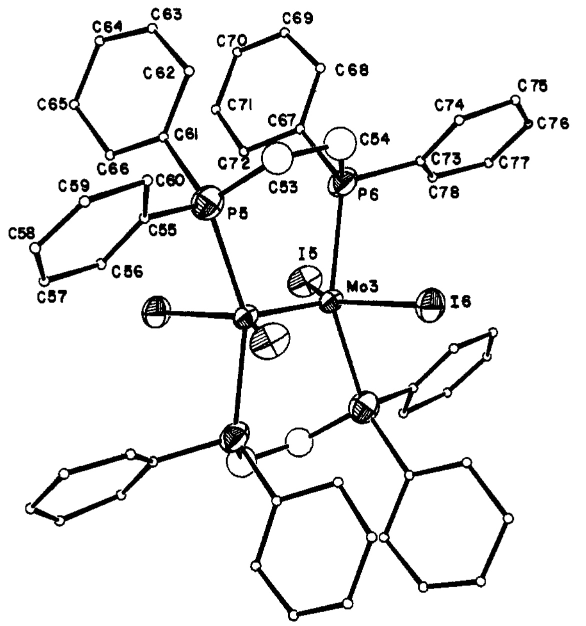

Figure 3. Structure and labeling scheme for the eclipsed molecule, **1b**, in β-$Mo_2I_4(dppe)_2\cdot{}^2/_3CH_2Cl_2$ (**1**). Atoms are represented by their 50% probability ellipsoids. The midpoint of the Mo–Mo axis resides on an inversion center.

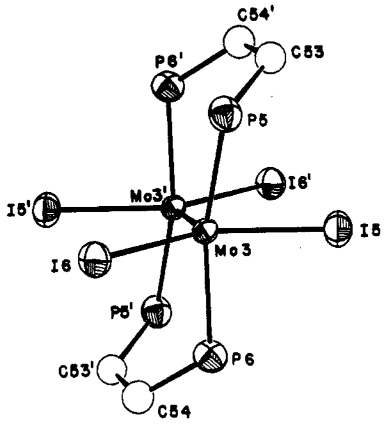

Figure 4. Partial ORTEP plot of molecule **1b** viewed down the Mo(3)–Mo(3)′ axis.

occupies the twofold centrosymmetric special position and has an eclipsed conformation ($\chi = 0$). Form **2** contains only one set of equivalent molecules, which are twisted, with $\chi = 25.7°$.

The structure of molecule **1a** is shown in Figure 1, where the complete atom-labeling scheme is also given. Figure 2 gives an informative view of the rotational conformation of molecule **1a**. From this view, which is straight down the Mo–Mo bond, the twisting of the molecule is evident. The idealized symmetry of this skeletal set of atoms is D_2. While the molecule shown has a counterclockwise twist, it must be remembered that in each unit cell there are four twisted molecules, two of each chirality. Each six-membered ring has a twist–chair conformation; in a simple chair conformation the C–C and Mo–Mo bonds would be parallel, and it is clear from Figure 2 that they are not. The principal molecules in the disordered structures[1,3,17] of β-$Mo_2Cl_4(dppe)_2$ and β-$Mo_2Br_4(dppe)_2$ have essentially this same type of ring conformation.

For the molecule of type **1b** we have a centrosymmetric structure of a type never previously seen in a $M_2X_4(dppe)_2$ type molecule. Figure 3 presents a labeled ORTEP diagram of the complete molecule, and Figure 4 shows the important central region in a perspective that emphasizes the eclipsed structure and the ring conformations. While the exact crystallographic symmetry is only $\bar{1}$, the skeleton shown in Figure 4 has effectively $2/m$ (C_{2h}) symmetry.

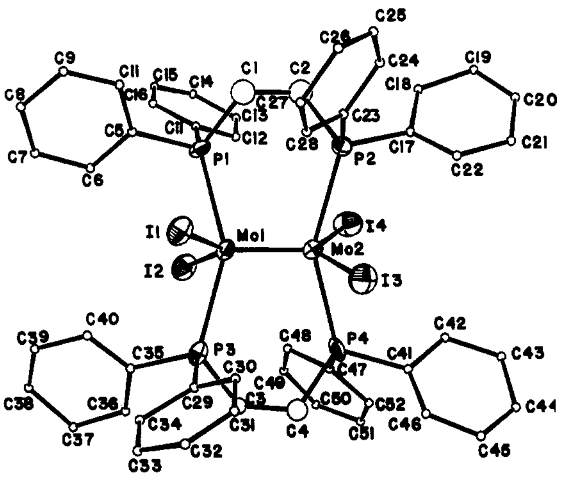

Figure 5. Drawing of the molecule in β'-$Mo_2I_4(dppe)_2\cdot C_7H_8$ showing the atom-labeling scheme. Phenyl groups are represented by small circles, and other atoms are represented by their 50% probability ellipsoids.

In compound **2**, all of the molecules of β-$Mo_2I_4(dppe)_2$ are of one type and are found on the general, fourfold equipoint of space group $P2_1/n$. These molecules, shown in Figure 5, are very similar to the **1a** molecules although they have a slightly different mean torsion angle, 25.7°, instead of 27.9°. The independent torsion angles used to calculate the average χ values in **1a** and **2** are listed in Table IV.

In neither **1a** nor **2** is there any evidence for the type of disorder that often occurs in crystalline $M_2X_4(dppe)_2$ compounds,[1,3,17] wherein a small fraction of the molecules are oriented perpendicular to the majority, giving a near overlap of ligand atoms but entailing a markedly different conformation of the six-membered rings. The absence of such a disorder in the present cases is probably due to the large size of the iodine atoms and the great difference between the Mo–I and Mo–P bond lengths (as compared to the chloro and bromo cases), thus leading to a much poorer match of the secondary orientation to the site defined by the major one.

The simultaneous presence of the two types of molecules in **1** must be due to the fact that the boat conformation of the rings in **1b**, is only moderately unfavorable relative to the twist–chair conformations in **1a**. Since the twist–chair conformations can be achieved only at the expense of some of the δ bond energy, the net stability difference between **1a** and **1b** evidently becomes so small that intermolecular packing forces can assume a decisive role in stabilizing each one at a different site. This is a circumstance that will probably not occur often, but it is one that can be taken advantage of in spectroscopic studies, as shown below.

On the whole, the structures of the three molecules, **1a**, **1b**, and **2**, vary little with respect to metal–ligand distances and bond angles, as can be seen in Table III. For example, for the molecules in the above order, the mean Mo–I distances are 2.74 [4], 2.748 [6], and 2.732 [3] Å. The greatest variation occurs in the I–Mo–I angles, which are (in the same order) 138 [2], 143.1 (1), and 134.5 [7]°. Table V lists important average bond distances and angles for **1** and **2**.

With respect to the Mo–Mo distance, there are differences, and these are of key interest because of their relationship to the dependence of δ bond strength on the angle of internal rotation. The previous correlations of the Mo–Mo distance with the angle χ employed a series of compounds all having different compositions.[7] The present study provides a check on the previous assumption that composition per se has a negligible effect on the Mo–Mo distance.

Turning first to the two twisted molecules, **1a** and **2**, the mean torsion angles, 27.9 [8] and 25.7 [6]°, respectively, differ by an amount that is barely at the threshold of statistical significance, viz. 2.2 (7)°. It is therefore not surprising that there is no significant difference between the Mo–Mo bond lengths in these two molecules, which are 2.180 (4) and 2.179 (3) Å. However,

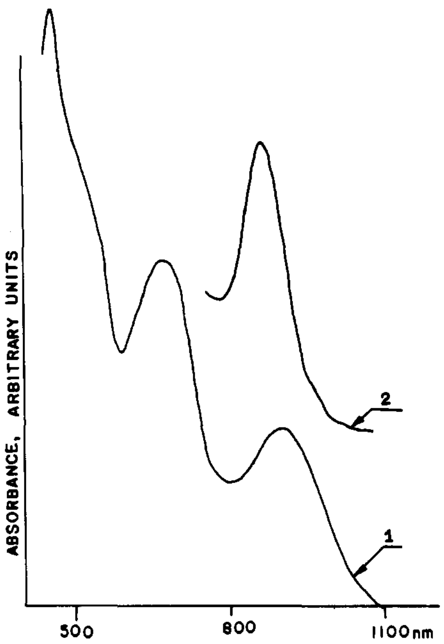

Figure 6. Visible spectra of β-$Mo_2I_4(dppe)_2 \cdot {}^2/_3CH_2Cl_2$ (**1**) and β′-$Mo_2I_4(dppe)_2 \cdot C_7H_8$ (**2**) recorded on Nujol mull samples.

molecule **1b**, with a mean torsion angle of zero, is much shorter. The Mo–Mo distance here, 2.129 (5) Å, is 0.050 (6) Å shorter than the average value for a mean torsion angle of 26.8 ± 1.1°.

From the difference of 0.050 (6) Å for a change of torsion angles from 0 to 26.89 ± 1.1°, we can estimate the change in Mo–Mo bond length that would occur if the torsion angle were increased to 45°; this is the same as estimating the total bond shortening contributed by the presence of the δ bond and has been estimated before.[7] We do this by assuming, as before, a linear dependence of Mo–Mo bond length on cos (2χ). This leads to a total change of 0.085 ± 0.05 Å, which is reasonably close to the value of 0.097 Å obtained previously.

Electronic Spectra. The availability of the "same" $Mo_2X_4(LL)_2$ molecule fixed, by its crystalline environment, in three different rotational conformations provides a special opportunity to see how well our theoretical picture of the M–M bonding can account for the experimental dependence of the δ → δ* spectrum upon the rotational angle. Actually, two aspects of the spectrum can be considered, viz. the band position and the band intensity. The spectra were recorded on the two crystalline compounds, **1** and **2**, by mulling them in mineral oil, in much the same way as is done more commonly for recording infrared spectra of solids, except that more attention must be given to having very small particles, so as to minimize reflective scattering.

The spectra are shown in Figure 6. It is clear that the spectrum of **1** shows two well-separated bands, in accord with the fact that there are two distinct rotamers present. The spectrum of **2** displays only one δ → δ* band. The positions of the band maxima can be summarized as follows: **1a**, λ = 920 nm, ν = 10 900 cm^{-1}; **1b**, λ = 670 nm, ν = 14 900 cm^{-1}; **2**, λ = 878 nm, ν = 11 400 cm^{-1}.

The assignment of the two peaks in the spectrum of compounds **1** to **1a** and **1b** in the manner shown assumes that the molecule with the more twisted conformation will have the lower energy absorption band and is based on the general correlations previously published[5] for β-$Mo_2X_4(LL)_2$ compounds with X = Cl or Br.

Figure 7 shows the spectrum of β-$Mo_2I_4(dppe)_2$ in dichloromethane solution. Here the δ–δ* band is found at λ_{max} = 860 nm (ν = 11 600 cm^{-1}) with an ϵ_{max} value of 2000 M^{-1} cm^{-1}. This suggests that the molecule adopts a twisted rotational conformation in solution with a mean torsion angle (χ) similar to those in **1a** and **2**, namely, about 27°.

We can now compare the dependence of the δ → δ* transition energy on the angle of internal rotation for the iodine compounds with previous results concerning analogous chloro and bromo compounds.[5] In Figure 8 we show the previous results along with the new ones for the iodo systems. In addition to the data from the crystal spectra for compounds **1** and **2** reported here, we also include a point for the compound $Mo_2I_4(dppm)_2$, which has only recently been reported.[18] With so few points it is not possible to determine independently the best sort of curve to relate the two parameters. The one drawn is simply chosen to be as similar as possible to the curves for the chloro and bromo compounds.

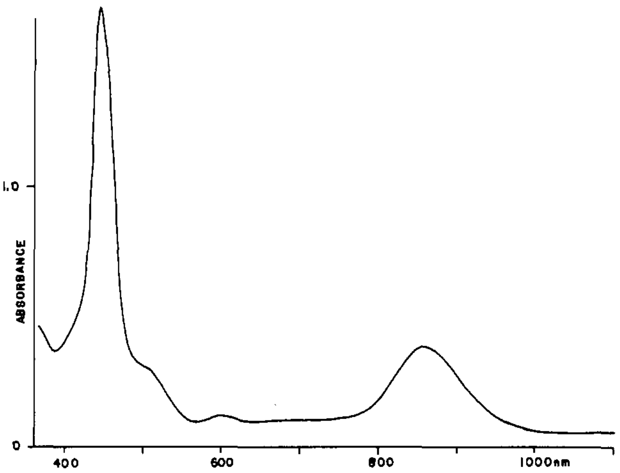

Figure 7. UV–visible spectrum of β-$Mo_2I_4(dppe)_2 \cdot {}^2/_3CH_2Cl_2$ in dichloromethane solution.

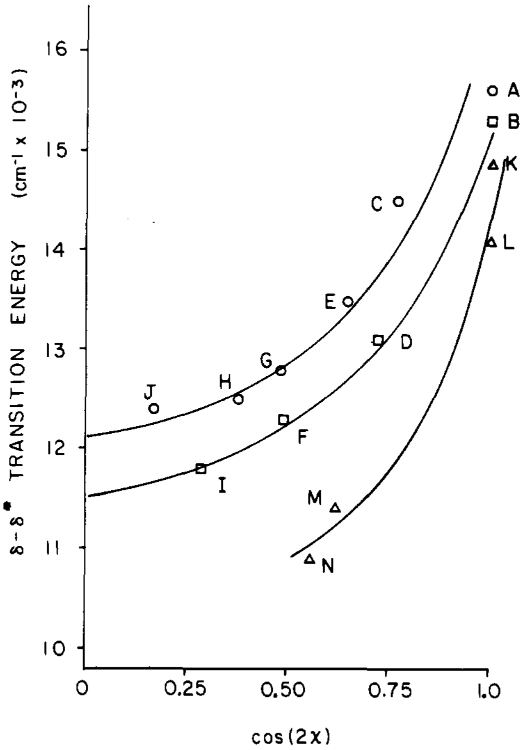

Figure 8. Plot of δ → δ* transition energies for fourteen $Mo_2X_4(PP)_2$ compounds. Points A–J are for compounds with X = Cl and Br. Individual compounds are identified in the corresponding plot in ref 5. The iodo compounds shown here are as follows: (K) $Mo_2I_4(dppe)_2$, with χ = 0°; (L) $Mo_2I_4(dppm)_2$, with χ = 0° (data from ref 18); (M) $Mo_2I_4(dppe)_2$, with χ = 25.7°; (N) $Mo_2I_4(dppe)_2$, with χ = 27.9°.

It is in comparing the intensities of the two bands in the spectrum of compound **1** that we have here a unique opportunity. To make an appropriate comparison, the spectrum was replotted on a linear energy scale with a correction for the rising base line. Part of this rise may well be real, resulting from the onset of strong UV absorption, but to a considerable extent it is due to the increasing reflective scattering by the small particles as the wavelength of the radiation becomes shorter. In any event, from a suitably replotted spectrum with a flat base line and a linear

Table II. Atomic Positional Parameters and Equivalent Isotropic Displacement Parameters and Their Estimated Standard Deviations for $Mo_2I_4(dppe)_2\cdot{}^2/_3\ CH_2Cl_2$ (**1**) and $Mo_2I_4(dppe)_2\cdot C_7H_8$ (**2**)[a]

Compound **1**

atom	*x*	*y*	*z*	*B*, Å^2	atom	*x*	*y*	*z*	*B*, Å^2
Mo(1)	0.7354 (2)	0.5113 (2)	0.16968 (7)	2.33 (6)	C(39)	0.705 (3)	0.826 (2)	0.106 (1)	4.5 (8)*
Mo(2)	0.8836 (2)	0.5512 (2)	0.16341 (7)	2.25 (6)	C(40)	0.756 (2)	0.761 (2)	0.1256 (8)	3.0 (7)*
I(1)	0.7536 (2)	0.3973 (1)	0.22238 (6)	3.61 (5)	C(41)	0.715 (2)	0.583 (2)	0.2754 (8)	2.8 (6)*
I(2)	0.5916 (2)	0.5907 (1)	0.12241 (6)	3.88 (5)	C(42)	0.655 (3)	0.622 (2)	0.2993 (9)	4.0 (8)*
I(3)	0.8904 (2)	0.6081 (1)	0.09184 (6)	3.60 (5)	C(43)	0.688 (3)	0.620 (2)	0.339 (1)	4.6 (8)*
I(4)	1.0162 (2)	0.5328 (1)	0.22929 (6)	3.49 (5)	C(44)	0.771 (3)	0.592 (2)	0.355 (1)	4.9 (8)*
P(1)	0.6948 (6)	0.4057 (5)	0.1197 (2)	2.6 (2)	C(45)	0.838 (2)	0.556 (2)	0.3328 (9)	3.8 (8)*
P(2)	0.9647 (6)	0.4326 (5)	0.1361 (2)	2.7 (2)	C(46)	0.808 (2)	0.553 (2)	0.2910 (9)	3.9 (7)*
P(3)	0.8795 (7)	0.6903 (5)	0.1861 (2)	3.1 (2)	C(47)	0.542 (2)	0.581 (2)	0.2184 (9)	3.6 (7)*
P(4)	0.6781 (6)	0.5915 (5)	0.2227 (2)	3.1 (2)	C(48)	0.512 (3)	0.511 (2)	0.234 (1)	4.9 (9)*
C(1)	0.803 (2)	0.337 (2)	0.1163 (9)	3.1 (7)*	C(49)	0.404 (4)	0.499 (3)	0.228 (2)	11 (2)*
C(2)	0.877 (2)	0.380 (2)	0.0993 (9)	3.5 (7)*	C(50)	0.343 (3)	0.564 (2)	0.215 (1)	6 (1)*
C(3)	0.813 (2)	0.709 (2)	0.2282 (9)	3.5 (7)*	C(51)	0.379 (3)	0.630 (2)	0.203 (1)	5.0 (9)*
C(4)	0.703 (2)	0.696 (2)	0.2177 (8)	3.1 (7)*	C(52)	0.478 (3)	0.639 (2)	0.2026 (9)	4.1 (8)*
C(5)	0.650 (2)	0.419 (2)	0.0690 (8)	2.6 (6)*	Mo(3)	0.0585 (2)	0.0264 (2)	0.01879 (7)	2.20 (6)
C(6)	0.670 (2)	0.484 (2)	0.0489 (8)	2.4 (6)*	I(5)	−0.0192 (2)	0.0888 (1)	0.07927 (6)	3.91 (5)
C(7)	0.641 (2)	0.490 (2)	0.0085 (8)	2.5 (6)*	I(6)	0.2304 (2)	0.0119 (1)	−0.01236 (6)	3.66 (5)
C(8)	0.583 (3)	0.434 (2)	−0.009 (1)	4.5 (8)*	P(5)	0.1247 (6)	−0.0713 (5)	0.0728 (2)	2.7 (2)
C(9)	0.565 (3)	0.367 (2)	0.010 (1)	4.5 (8)*	P(6)	0.0554 (6)	0.1565 (5)	−0.0110 (2)	2.5 (2)
C(10)	0.594 (2)	0.360 (2)	0.0488 (9)	3.3 (7)*	C(53)	0.016 (2)	−0.116 (2)	0.0915 (9)	3.4 (7)*
C(11)	0.592 (2)	0.348 (2)	0.1351 (7)	1.8 (6)*	C(54)	0.063 (3)	0.161 (2)	−0.0634 (9)	3.8 (7)*
C(12)	0.503 (2)	0.383 (2)	0.1363 (9)	3.5 (7)*	C(55)	0.190 (2)	−0.018 (2)	0.1140 (9)	3.7 (7)*
C(13)	0.424 (2)	0.344 (2)	0.1495 (8)	3.2 (7)*	C(56)	0.251 (3)	0.034 (2)	0.105 (1)	5.0 (9)*
C(14)	0.435 (2)	0.268 (2)	0.1579 (9)	3.7 (7)*	C(57)	0.309 (3)	0.080 (2)	0.136 (1)	5.2 (9)*
C(15)	0.525 (3)	0.234 (2)	0.158 (1)	5.0 (9)*	C(58)	0.297 (4)	0.069 (3)	0.174 (1)	8 (1)*
C(16)	0.611 (3)	0.273 (2)	0.147 (1)	5 (1)*	C(59)	0.236 (3)	0.016 (3)	0.178 (1)	8 (1)*
C(17)	1.067 (2)	0.460 (2)	0.1125 (7)	1.7 (5)*	C(60)	0.170 (3)	−0.033 (2)	0.151 (1)	5.5 (9)*
C(18)	1.148 (2)	0.493 (2)	0.1350 (9)	4.0 (8)*	C(61)	0.219 (2)	−0.149 (2)	0.0729 (8)	2.6 (6)*
C(19)	1.235 (3)	0.511 (3)	0.118 (1)	7 (1)*	C(62)	0.191 (3)	−0.223 (2)	0.085 (1)	4.4 (8)*
C(20)	1.237 (3)	0.496 (2)	0.081 (1)	5.0 (9)*	C(63)	0.267 (3)	−0.276 (2)	0.086 (1)	4.1 (8)*
C(21)	1.159 (3)	0.459 (2)	0.058 (1)	4.4 (8)*	C(64)	0.358 (3)	−0.262 (2)	0.080 (1)	5.3 (9)*
C(22)	1.072 (2)	0.444 (2)	0.0737 (9)	3.2 (7)*	C(65)	0.388 (3)	−0.188 (2)	0.069 (1)	6 (1)*
C(23)	1.021 (2)	0.350 (2)	0.1646 (8)	2.7 (6)*	C(66)	0.309 (3)	−0.129 (2)	0.0641 (9)	4.0 (8)*
C(24)	1.075 (3)	0.303 (2)	0.144 (1)	5.0 (9)*	C(67)	−0.037 (2)	0.229 (2)	−0.0024 (8)	2.8 (6)*
C(25)	1.115 (2)	0.238 (2)	0.1644 (9)	3.5 (7)*	C(68)	−0.018 (3)	0.304 (2)	−0.012 (1)	4.4 (8)*
C(26)	1.097 (3)	0.220 (2)	0.201 (1)	4.4 (8)*	C(69)	−0.092 (3)	0.354 (2)	−0.0079 (9)	4.1 (8)*
C(27)	1.048 (3)	0.275 (2)	0.220 (1)	5.1 (9)*	C(70)	−0.177 (3)	0.335 (2)	0.0042 (9)	4.1 (8)*
C(28)	1.005 (3)	0.335 (2)	0.203 (1)	4.8 (9)*	C(71)	−0.199 (2)	0.261 (2)	0.0119 (9)	3.8 (8)*
C(29)	1.005 (2)	0.724 (2)	0.2004 (8)	2.6 (6)*	C(72)	−0.131 (2)	0.203 (2)	0.0073 (9)	3.1 (7)*
C(30)	1.065 (3)	0.725 (2)	0.1735 (9)	3.9 (8)*	C(73)	0.169 (2)	0.207 (2)	0.0095 (7)	1.9 (6)*
C(31)	1.168 (3)	0.759 (2)	0.184 (1)	5.4 (9)*	C(74)	0.228 (3)	0.240 (2)	−0.015 (1)	6 (1)*
C(32)	1.196 (3)	0.790 (2)	0.219 (1)	5.0 (9)*	C(75)	0.309 (3)	0.289 (2)	0.006 (1)	5.0 (9)*
C(33)	1.134 (3)	0.782 (2)	0.246 (1)	6 (1)*	C(76)	0.331 (3)	0.293 (2)	0.044 (1)	6 (1)*
C(34)	1.035 (3)	0.755 (2)	0.239 (1)	4.8 (9)*	C(77)	0.268 (3)	0.258 (2)	0.067 (1)	5.5 (9)*
C(35)	0.830 (2)	0.771 (2)	0.1572 (9)	3.0 (7)*	C(78)	0.182 (3)	0.219 (2)	0.048 (1)	4.9 (9)*
C(36)	0.859 (3)	0.843 (2)	0.1674 (9)	4.1 (8)*	C(79)	0.463 (7)	0.105 (6)	0.047 (3)	21 (4)*
C(37)	0.815 (3)	0.906 (2)	0.146 (1)	5.0 (9)*	Cl(1)	0.508 (2)	0.018 (1)	0.0673 (6)	15*
C(38)	0.741 (3)	0.892 (2)	0.1166 (9)	4.3 (8)*	Cl(2)	0.555 (2)	0.155 (1)	0.0346 (6)	15.8 (5)*

Compound **2**

atom	*x*	*y*	*z*	*B*, Å^2	atom	*x*	*y*	*z*	*B*, Å^2
Mo(1)	0.8418 (3)	0.2240 (1)	0.1598 (2)	1.89 (5)	C(13)	1.296 (4)	0.203 (2)	0.249 (2)	5 (1)*
Mo(2)	0.8352 (3)	0.1370 (1)	0.1556 (2)	1.92 (5)	C(14)	1.360 (3)	0.248 (2)	0.275 (2)	3.5 (8)*
I(1)	0.6746 (2)	0.2673 (1)	0.2278 (1)	3.04 (5)	C(15)	1.308 (3)	0.289 (2)	0.298 (2)	4 (1)*
I(2)	1.0157 (2)	0.2662 (1)	0.0964 (1)	3.02 (5)	C(16)	1.183 (3)	0.290 (2)	0.292 (2)	4.3 (9)*
I(3)	0.6243 (2)	0.0985 (1)	0.1648 (1)	3.38 (6)	C(17)	0.910 (3)	0.037 (1)	0.291 (2)	2.6 (7)*
I(4)	1.0389 (2)	0.0929 (1)	0.1403 (1)	3.36 (6)	C(18)	1.018 (4)	0.022 (2)	0.326 (2)	5 (1)*
P(1)	0.9708 (8)	0.2446 (4)	0.2709 (4)	2.3 (2)	C(19)	1.040 (4)	−0.035 (2)	0.344 (2)	6 (1)*
P(2)	0.8727 (9)	0.1060 (4)	0.2843 (4)	2.5 (2)	C(20)	0.959 (4)	−0.070 (2)	0.319 (2)	6 (1)*
P(3)	0.7175 8)	0.2561 (4)	0.0513 (5)	2.6 (2)	C(21)	0.854 (4)	−0.058 (2)	0.283 (2)	5 (1)*
P(4)	0.7942 (8)	0.1163 (3)	0.0248 (5)	2.2 (2)	C(22)	0.838 (3)	−0.004 (2)	0.270 (2)	3.9 (9)*
C(1)	0.958 (3)	0.199 (1)	0.345 (2)	2.7 (7)*	C(23)	0.769 (3)	0.109 (1)	0.345 (2)	2.0 (7)*
C(2)	0.987 (3)	0.142 (1)	0.337 (2)	2.6 (7)*	C(24)	0.774 (3)	0.074 (1)	0.406 (2)	3.4 (8)*
C(3)	0.727 (2)	0.218 (1)	−0.029 (1)	1.0 (6)*	C(25)	0.700 (4)	0.084 (2)	0.456 (2)	6 (1)*
C(4)	0.683 (3)	0.161 (1)	−0.026 (2)	1.9 (6)*	C(26)	0.623 (4)	0.119 (2)	0.451 (2)	5 (1)*
C(5)	0.937 (3)	0.310 (2)	0.305 (2)	3.2 (8)*	C(27)	0.608 (3)	0.154 (2)	0.392 (2)	4.2 (9)*
C(6)	0.946 (3)	0.353 (1)	0.258 (2)	3.1 (8)*	C(28)	0.689 (2)	0.146 (1)	0.341 (2)	2.1 (7)*
C(7)	0.920 (3)	0.406 (2)	0.287 (2)	4.4 (9)*	C(29)	0.562 (3)	0.261 (2)	0.050 (2)	3.3 (8)*
C(8)	0.885 (3)	0.414 (2)	0.354 (2)	3.9 (9)*	C(30)	0.504 (3)	0.223 (2)	0.076 (2)	3.2 (8)*
C(9)	0.882 (4)	0.371 (2)	0.397 (2)	5 (1)*	C(31)	0.379 (4)	0.226 (2)	0.072 (2)	5 (1)*
C(10)	0.905 (3)	0.319 (1)	0.373 (2)	2.4 (7)*	C(32)	0.334 (3)	0.271 (2)	0.047 (2)	5 (1)*
C(11)	1.121 (3)	0.247 (2)	0.273 (2)	3.6 (8)*	C(33)	0.395 (4)	0.314 (2)	0.022 (2)	5 (1)*
C(12)	1.177 (3)	0.205 (1)	0.244 (2)	2.5 (7)*	C(34)	0.514 (3)	0.313 (2)	0.025 (2)	4.1 (9)*

Table II (Continued)

atom	x	y	z	B, Å^2	atom	x	y	z	B, Å^2
C(35)	0.755 (2)	0.323 (1)	0.025 (2)	1.7 (6)*	C(48)	0.990 (3)	0.160 (1)	−0.026 (2)	2.6 (7)*
C(36)	0.776 (3)	0.332 (2)	−0.042 (2)	4 (1)*	C(49)	1.058 (3)	0.163 (1)	−0.079 (2)	2.8 (7)*
C(37)	0.797 (4)	0.386 (2)	−0.068 (2)	6 (1)*	C(50)	1.057 (3)	0.129 (2)	−0.135 (2)	4.1 (9)*
C(38)	0.809 (4)	0.428 (2)	−0.010 (2)	5 (1)*	C(51)	0.982 (3)	0.084 (2)	−0.142 (2)	3.8 (9)*
C(39)	0.778 (4)	0.417 (2)	0.053 (2)	6 (1)*	C(52)	0.903 (3)	0.079 (2)	−0.089 (2)	3.8 (9)*
C(40)	0.764 (3)	0.363 (2)	0.072 (2)	4.2 (9)*	C(53)	0.665 (5)	0.070 (3)	0.674 (3)	10 (2)*
C(41)	0.737 (3)	0.048 (1)	0.007 (2)	1.7 (6)*	C(54)	0.214 (5)	0.461 (2)	0.233 (3)	8 (2)*
C(42)	0.812 (3)	0.007 (2)	0.028 (2)	3.2 (8)*	C(55)	0.349 (4	0.013 (2)	0.267 (3)	7 (1)*
C(43)	0.783 (4)	−0.048 (2)	0.004 (2)	6 (1)*	C(56)	0.449 (5)	0.025 (3)	0.315 (3)	9 (2)
C(44)	0.678 (4)	−0.054 (2)	−0.038 (2)	6 (1)*	C(57)	0.459 (6)	−0.010 (3)	0.366 (4)	13 (2)*
C(45)	0.611 (4)	−0.015 (2)	−0.055 (2)	5 (1)*	C(58)	0.577 (6)	0.058 (3)	0.625 (3)	10 (2)*
C(46)	0.641 (3)	0.037 (1)	−0.028 (2)	2.3 (7)*	C(59)	0.712 (9)	0.113 (4)	0.674 (5)	7 (3)*
C(47)	0.905 (3)	0.120 (1)	−0.035 (2)	2.4 (7)*	C(60)	0.33 (1)	0.053 (5)	0.235 (7)	11 (4)*

[a] Starred values denote isotropically refined atoms. B values for anisotropically refined atoms are given in the form of the isotropic equivalent thermal parameter defined as $(4/3)[a^2B(1,1) + b^2B(2,2) + c^2B(3,3) + ab(\cos\gamma)B(1,2) + ac(\cos\beta)B(1,3) + bc(\cos\alpha)B(2,3)]$.

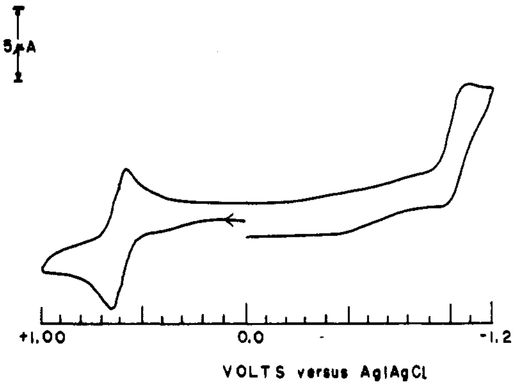

Figure 9. Cyclic voltammogram of β-$Mo_2I_4(dppe)_2$ in 0.2 M TBAH-dichloromethane at 200 mV/s at a Pt electrode.

frequency scale, the ratio of the two absorption band intensities, I_a and I_b, can be evaluated as the ratio of the areas under the two bands. This ratio was found to be 0.40 ± 0.04. We must also note that by its composition, compound **1** provides two **1a** chromophores per **1b** chromophore. Let us now see how this compares with expectation from theory.

The δ overlap is a weak overlap and, as pointed out a long time ago by Trogler and Gray,[20] the intensity of the $\delta \rightarrow \delta^*$ transition might well be expected to display a proportionality to the square of the orbital overlap, according to a limiting relationship first derived by Mulliken.[21] No quantitative test of this proposal has heretofore been possible, because no two chromophores differing only in the magnitude of the overlap and in fixed molar ratio have been available. With the two rotamers in compound **1**, such a pair is now available. The difference in overlap in the two rotamers is primarily determined by the different angles of rotation, although a secondary factor will be the difference in bond lengths.

On going from molecule **1b** ($\chi = 0°$) to molecule **1a** ($\chi = 27.9°$), the δ overlap will decrease by a factor of $\cos^2 (2 \times 27.9°) = 0.316$. Thus, the intensity should decrease by a little more than this because the increase in bond length, from 2.129 (5) to 2.180 (4) Å will cause a further small loss of overlap. However, since there are twice as many **1a** molecules as **1b** molecules, the observed intensity ratio should be reduced by only half this amount, thus giving a ratio I_a/I_b of <0.63. We have no good way of estimating how much of an effect the increased Mo–Mo distance will have, but it is unlikely to lower the predicted ratio to less than 0.5. Thus, the predicted and observed ratios, 0.5–0.6 and ca. 0.40, respectively, are in approximate agreement. It should be remembered that the postulated dependence of intensity on the square of the overlap is only an approximate relationship, so that there is no reason to expect exact agreement with experiment.

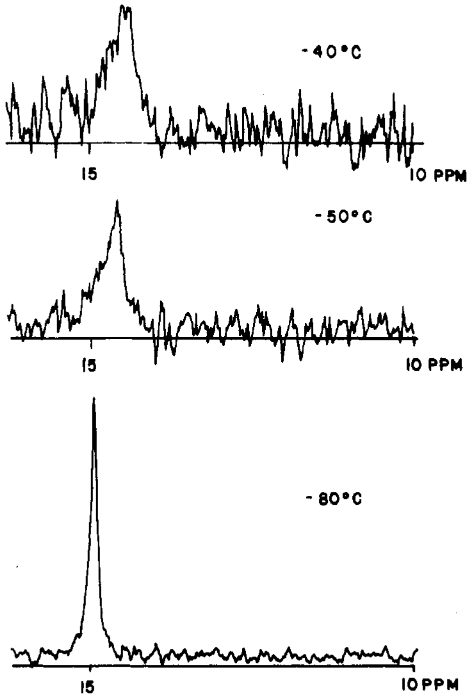

Figure 10. $^{31}P\{^1H\}$ NMR spectrum of β-$Mo_2I_4(dppe)_2 \cdot {}^2/_3CH_2Cl_2$ in dichloromethane-d_2 over the temperature range −40 to −80 °C: (a) −40 °C, (b) −50 °C, (c) −80 °C.

Electrochemical and ^{31}P NMR Studies. The electrochemical properties of β-$Mo_2I_4(dppe)_2$ were studied by using the cyclic voltammetry technique. The compound exhibits a reversible one-electron oxidation at an $E_{1/2}$ of +0.62 V vs. Ag/AgCl, as shown in Figure 9. The potential separation between the anodic and cathodic peaks, ΔE_p, is ~70 mV for a sweep rate of 200 mV/s and $i_{p,c}/i_{p,a} \sim 1$. An irreversible reduction occurs at about ~−1.04 V. These are, presumably, metal-based redox processes, corresponding to the removal of an electron from the δ-bonding orbital (oxidation) and to the placement of an electron in the δ^*-antibonding orbital (reduction). Both events cause the formal bond order to decrease by 0.5 from 4.0 to 3.5.

The electrochemistry of the title compound is similar to the redox behavior of other quadruply bonded dimolybdenum compounds that contain halide and phosphine ligands.[22] A particularly relevant comparison in this case is with the compounds β-$Mo_2Cl_4(dppe)_2$ and β-$Mo_2Br_4(dppe)_2$, which exhibit a one-electron

---

(20) Trogler, W. C.; Gray, H. B. *Acc. Chem. Res.* **1978**, *11*, 232.

(21) Mulliken, R. S. *J. Chem. Phys.* **1939**, *7*, 20.

(22) (a) Zietlow, T.; Gray, H. B. Presented at the 187th National meeting of the American Chemical Society, St. Louis, MO, April 11, 1984; paper INOR 197. (b) Zietlow, T.; Klendworth, D. D.; Nimry, T.; Salmon, D. J.; Walton, R. A. *Inorg. Chem.* **1981**, *20*, 947.

(23) Agaskar, P. A., private communication.

Table III. Selected Bond Distances (Å) and Angles (deg) for $Mo_2I_4(dppe)_2 \cdot {}^2/_3 CH_2Cl_2$ (**1**) and $Mo_2I_4(dppe)_2 \cdot C_7H_8$ (**2**)[a]

Compound **1**

atom 1	atom 2	dist	atom 1	atom 2	dist	atom 1	atom 2	dist
Mo(1)	Mo(2)	2.180 (4)	Mo(3)	I(5)	2.755 (3)	P(1)	C(1)	1.92 (3)
Mo(1)	I(1)	2.735 (3)	Mo(3)	I(6)	2.742 (3)	P(2)	C(2)	1.88 (3)
Mo(1)	I(2)	2.757 (3)	Mo(3)	P(5)	2.633 (8)	P(3)	C(3)	1.88 (3)
Mo(1)	P(1)	2.576 (8)	Mo(3)	P(6)	2.536 (8)	P(4)	C(4)	1.91 (3)
Mo(1)	P(4)	2.565 (8)	P(5)	C(53)	1.88 (3)	C(11)	C(2)	1.46 (4)
Mo(2)	I(3)	2.736 (3)	P(6)	C(54)	1.87 (3)	C(3)	C(4)	1.50 (4)
Mo(2)	I(4)	2.737 (3)	C(53)	C(54)	1.57 (4)	Mo(3)	Mo(3)′	2.129 (5)
Mo(2)	P(2)	2.627 (8)	Mo(2)	P(3)	2.599 (9)			

atom 1	atom 2	atom 3	angle	atom 1	atom 2	atom 3	angle
Mo(2)	Mo(1)	I(1)	108.6 (1)	Mo(2)	P(2)	C(2)	113 (1)
Mo(2)	Mo(1)	I(2)	110.8 (1)	Mo(2)	P(3)	C(3)	116 (1)
Mo (2)	Mo(1)	P(1)	105.8 (2)	Mo(1)	P(4)	C(4)	113.3 (9)
Mo(2)	Mo(1)	P(4)	106.4 (2)	P(1)	C(1)	C(2)	106 (2)
I(1)	Mo(1)	I(2)	140.6 (1)	P(2)	C(2)	C(1)	112 (2)
I(1)	Mo(1)	P(1)	85.1 (2)	P(3)	C(3)	C(4)	111 (2)
I(1)	Mo(1)	P(4)	85.5 (2)	P(4)	C(4)	C(3)	108 (2)
I(2)	Mo(1)	P(1)	84.2 (2)	Mo(3)	Mo(3)′	I(5)	108.8 (2)
I(2)	Mo(1)	P(4)	83.8 (2)	Mo(3)	Mo(3)′	I(6)	108.1 (2)
P(1)	Mo(1)	P(4)	147.8 (3)	Mo(3)	Mo(3)′	P(5	107.6 (2)
Mo(1)	Mo(2)	I(3)	112.0 (1)	Mo(3)	Mo(3)′	P(6)	100.3 (2)
Mo(1)	Mo(2)	I(4)	112.0 (1)	I(5)	Mo(3)	I(6)	143.1 (1)
Mo(1)	Mo(2)	P(2)	102.9 (2)	I(5)	Mo(3)	P(5)	80.4 (2)
Mo(1)	Mo(2)	P(3)	102.4 (2)	I(5)	Mo(3)	P(6)	88.4 (2)
I(3)	Mo(2)	I(4)	135.9 (1)	I(6)	Mo(3)	P(5)	90.6 (2)
I(3)	Mo(2)	P(2)	83.2 (2)	I(6)	Mo(3)	P(6)	83.1 (2)
I(3)	Mo(2)	P(3)	86.5 (2)	P(5)	Mo(3)	P(6)	152.0 (3)
I(4)	Mo(2)	P(2)	87.5 (2)	Mo(3)	P(5)	C(53)	109 (1)
I(4)	Mo(2)	P(3)	83.9 (2)	Mo(3)	P(6)	C(54)	117 (1)
P(2)	Mo(2)	P(3)	154.7 (3)	P(5)	C(53)	C(54)	120 (2)
Mo(1)	P(1)	C(1)	115 (1)	P(6)	C(54)	C(53)	118 (2)

Compound **2**

atom 1	atom 2	dist	atom 1	atom 2	dist	atom 1	atom 2	dist
Mo(1)	Mo(2)	2.179 (3)	Mo(2)	I(3)	2.734 (4)	P(2)	C(2)	1.86 (3)
Mo(1)	I(1)	2.732 (4)	Mo(2)	I(4)	2.727 (4)	P(3)	C(3)	1.84 (3)
Mo(1)	I(2)	2.739 (4)	Mo(2)	P(2)	2.614 (9)	P(4)	C(4)	1.94 (3)
Mo(1)	P(1)	2.583 (8)	Mo(2)	P(4)	2.592 (9)	C(1)	C(2)	1.50 (4)
Mo(1)	P(3)	2.590 (9)	P(1)	C(1)	1.86 (3)	C(3)	C(4)	1.53 (4)

atom 1	atom 2	atom 3	angle	atom 1	atom 2	atom 3	angle
Mo(2)	Mo(1)	I(1)	112.9 (2)	Mo(1)	Mo(2)	P(2)	105.0 (3)
Mo(2)	Mo(1)	I(2)	113.3 (2)	Mo(1)	Mo(2)	P(4)	103.9 (2)
Mo(2)	Mo(1)	P(1)	104.4 (2)	I(3)	Mo(2)	I(4)	135.3 (1)
Mo(2)	Mo(1)	P(3)	105.3 (2)	I(3)	Mo(2)	P(2)	84.7 (2)
I(1)	Mo(1)	I(2)	133.8 (1)	I(3)	Mo(2)	P(4)	84.4 (2)
I(1)	Mo(1)	P(1)	85.9 (2)	I(4)	Mo(2)	P(2)	84.8 (2)
I(1)	Mo(1)	P(3)	82.9 (2)	I(4)	Mo(2)	P(4)	84.3 (2)
I(2)	Mo(1)	P(1)	82.8 (2)	P(2)	Mo(2)	P(4)	151.1 (3)
I(2)	Mo(1)	P(3)	85.4 (3)	P(1)	C(1)	C(2)	118 (2)
P(1)	Mo(1)	P(3)	150.3 (3)	P(2)	C(2)	C(1)	111 (2)
Mo(1)	Mo(2)	I(3)	112.4 (2)	P(3)	C(3)	C(4)	114 (2)
Mo(1)	Mo(2)	I(4)	112.3 (2)	P(4)	C(4)	C(3)	109 (2)

[a] Numbers in parentheses are estimated standard deviations in the least significant digits.

Table IV. Independent Torsion Angles (deg) for Molecules **1a** and **2**

molecule	plane 1	plane 2	angle
1a	I(1)–Mo(1)–Mo(2)	Mo(1)–Mo(2)–I(4)	29.24
	I(2)–Mo(1)–Mo(2)	Mo(1)–Mo(2)–I(3)	28.70
	P(1)–Mo(1)–Mo(2)	Mo(1)–Mo(2)–P(2)	26.70
	P(4)–Mo(1)–Mo(2)	Mo(1)–Mo(2)–P(3)	26.94
			χ_{av} = 27.9 [8]
2	I(1)–Mo(1)–Mo(2)	Mo(1)–Mo(2)–I(3)	25.50
	I(2)–Mo(1)–Mo(2)	Mo(1)–Mo(2)–I(4)	24.50
	P(1)–Mo(1)–Mo(2)	Mo(1)–Mo(2)–P(2)	26.60
	P(3)–Mo(1)–Mo(2)	Mo(1)–Mo(2)–P(4)	26.50
			χ_{av} = 25.7 [6]

Table V. Average Bond Distances (Å) and Angles (deg) for **1** and **2**[a]

	1a	**1b**	**2**
χ	27.9 (8)	0	25.7 (6)
Mo–I	2.74 [4]	2.748 [6]	2.732 [3]
Mo–P	2.59 [1]	2.58 [4]	2.594 [6]
P-C	1.85 [1]	1.86 [2]	1.84 [1]
Mo–Mo–I	110.8 [8]	108.4 [3]	112.7 [2]
Mo–Mo–P	104 [1]	103 [3]	104.6 [3]
I–Mo–I	138 [2]	143.1 (1)	134.5 [7]
P–Mo–P	151 [3]	152.0 (3)	150.7 [4]

[a] Numbers in brackets are variances, obtained from the expression $[\sum \Delta_i^2/n(n-1)]^{1/2}$, where Δ_i is the deviation of the *i*th value from the arithmetic mean and *n* is the total number of values averaged.

oxidation at $E_{1/2}$ values of +0.50 and +0.52 V, respectively.

^{31}P NMR Discussion. With the exception of the compounds $Mo_2X_4(dppm)_2$ (X = Cl, Br, I),[18,24] molecules of the type β-$Mo_2X_4(LL)_2$ have not been studied by NMR spectroscopy. Previous attempts to obtain ^{31}P NMR spectra of $Mo_2Cl_4(dppe)_2$ and $Mo_2Br_4(dppe)_2$ were unsuccessful.[23] Presumably the very low solubility of these complexes is responsible for the absence of any

---

(24) Harwood, W. S.; Qi, J.; Walton, R. A. *Polyhedron*, in press.

detectable signal within reasonable data acquisition times. With our recent synthesis of the more soluble iodo analogue, we were granted an opportunity to study the solution behavior of an $Mo_2X_4(dppe)_2$ compound using $^{31}P\{^1H\}$ spectroscopy.

Several $^{31}P\{^1H\}$ spectra of β-$Mo_2I_4(dppe)_2$ recorded at different temperatures are presented in Figure 10. There is no signal at room temperature, but as one cools the solution, a broad resonance appears between −30 and −40 °C, which becomes a sharp singlet as the temperature is lowered to −80 °C (Figure 10c). The resonance is located at +14.9 ppm, which is similar to the ^{31}P chemical shift values reported for $Mo_2X_4(dppm)_2$ compounds.[18,24] In the present study, the temperature dependence of the phosphorus resonance is indicative of a low-energy fluxional process that interconverts various rotational forms of the molecule. That such a process is occurring in solution is not surprising in view of the fact that several different rotational isomers are easily stabilized in the solid state. In structure **1**, the presence of both **1a**, with a twist-chair conformation, and **1b**, which exhibits a boat conformation of the rings, suggests that the energy differences are so small that weak intermolecular packing forces become important in determining the degree of twist that the molecules assume in the crystalline state.

Acknowledgment. We thank the National Science Foundation for financial support.

Registry No. **1**, 103852-10-4; **2**, 103957-54-6; $Mo_2(O_2CCH_3)_4$, 14221-06-8; Mo, 7439-98-7.

Supplementary Material Available: Full listings of bond angles, bond distances, and anisotropic displacement parameters (9 pages); tables of observed and calculated structure factors (37 pages). Ordering information is given on any current masthead page.

Contribution from the Department of Chemistry,
Purdue University, West Lafayette, Indiana 47907

Studies of the Photoinduced Ligand Substitution Reactions of $[Re(CNxyl)_6]^+$ (xyl = 2,6-Dimethylphenyl) in the Presence of Halide Ions

Nathan E. Stacy, Kay A. Conner, David R. McMillin,* and Richard A. Walton*

Received March 21, 1986

Irradiation of $[Re(CNxyl)_6]^+$ with UV light at 20 °C in dichloromethane and in the presence of halide ions yields complexes of the type $Re(CNxyl)_5X$, where X = Cl, Br, or I. The quantum yields are quite respectable, $\phi_P = 0.2$–0.3, and isolated product yields are in the range of 30–40%. The photoproducts have been characterized by spectroscopic methods and, in the case of the new derivatives $Re(CNxyl)_5Cl$ and $Re(CNxyl)_5Br$, by elemental microanalyses. The magnitudes of the quantum yields suggest that ligand substitution occurs by a dissociative mechanism involving a reactive d–d excited state.

Introduction

While isocyanide ligands are similar to carbon monoxide in that they may serve as σ donors and/or π acids,[1,2] available evidence suggests that isocyanides are better σ donors. Thus, there are several examples of isocyanide-containing complexes of metal ions in relatively high oxidation states, e.g., $[Cr(CNR)_7]^{2+}$,[3] $[Cr(CNR)_6]^{3+}$,[4] $[Mn(CNR)_6]^{2+}$,[5] and $[Mo(CNR)_7]^{2+}$[6,7] (R = alkyl and/or aryl), for which the isoelectronic carbonyl analogues are unknown. This means that a wider range of oxidation states can often be investigated for the isocyanide systems. In addition, the isocyanide function is versatile because the presence of the R group attached to nitrogen allows one to vary steric and electronic properties of the ligand very easily.

As photochemical methods have proved very useful in the synthesis of carbonyl complexes,[8,9] for example, in the synthesis of $Fe_2(CO)_9$,[10] they may be of importance in the preparation of isocyanide complexes as well, especially for those species that are not easily made by other routes.[11] As a case in point, we describe herein the photochemical generation of the complexes $Re(CNxyl)_5X$, where xylNC = 2,6-dimethylphenyl isocyanide and X is Cl, Br, or I. While Treichel and co-workers have reported a low-yield thermal route to the analogous $Re(CN$-p-$tol)_5X$ (X = Cl or Br) compounds by combining $Re(CO)_5X$ with p-tolyl isocyanide in refluxing toluene[12] and Cameron et al.[13] have shown that the iodo complex $Re(CNxyl)_5I$ can be prepared from K_2ReI_6, the most logical synthetic pathway is via the readily available homoleptic isocyanide cations $[Re(CNR)_6]^+$.[14,15] However, these 18-electron species are kinetically inert to ligand substitution reactions under thermal conditions, and some means of activation is therefore necessary. As shown below, photoinduced substitution of a xylyl isocyanide ligand of $[Re(CNxyl)_6]PF_6$ proceeds very cleanly in CH_2Cl_2, and the quantum efficiencies are rather high, $\phi_P \sim 0.2$.

Experimental Section

Starting Materials. $(n\text{-}Bu_4N)_2Re_2Cl_8$ was prepared by the method of Barder and Walton[16] and converted into $Re_2(O_2CCH_3)_4Cl_2$ according to the standard literature procedure[17] with a single important modification. The orange precipitate of $Re_2(O_2CCH_3)_4Cl_2$, which is formed after refluxing $(n\text{-}Bu_4N)_2Re_2Cl_8$ in CH_3COOH/acetic anhydride for 2 h, was too fine to be filtered conveniently and so had to be centrifuged, the supernatant decanted, and the solid washed successively with EtOH and Et_2O several times, centrifuging between each wash. The yield of product was 82%. The method of Cameron et al.[15] was used to prepare $[Re(CNxyl)_6]PF_6$ from $Re_2(O_2CCH_3)_4Cl_2$ with only minor changes as follows. Twenty milliliters of MeOH was added to a flask containing 0.48

---

(1) Malatesta, L.; Bonati, F. *Isocyanide Complexes of Metals*; Wiley: New York, 1969.
(2) Bonati, F.; Minghetti, G. *Inorg. Chim. Acta* **1974**, *9*, 95.
(3) Mialki, W. S.; Wigley, D. E.; Wood, T. E.; Walton, R. A. *Inorg. Chem.* **1982**, *21*, 480.
(4) Bohling, D. A.; Mann, K. R. *Inorg. Chem.* **1983**, *22*, 1561.
(5) See, for example: Nielson, R. M.; Wherland, S. *Inorg. Chem.* **1985**, *24*, 1803.
(6) Brant, P.; Cotton, F. A.; Sekutowski, J. C.; Wood, T. E.; Walton, R. A. *J. Am. Chem. Soc.* **1979**, *101*, 6588.
(7) Szalda, D. J.; Dewan, J. C.; Lippard, S. J. *Inorg. Chem.* **1981**, *20*, 3851.
(8) Koerner von Gustorf, E.; Grevels, F.-W. *Fortschr. Chem. Forsch.* **1969**, *13*, 366.
(9) Geoffroy, G. L.; Wrighton, M. S. *Organometallic Photochemistry*; Academic: New York, 1979; Chapter 2.
(10) Braye, E. H.; Hubel, W. *Inorg. Synth.* **1966**, *8*, 178.
(11) Previously, the most noteworthy photochemical studies have dealt with the excited-state reactivity patterns of the hexakis(aryl isocyanide) complexes of Cr(0), Mo(0), and W(0): Gray, H. B.; Mann, K. R.; Lewis, N. S.; Thich, J. A.; Richman, R. M. *Adv. Chem. Ser.* **1978**, *No. 168*, 44.
(12) Treichel, P. M.; Williams, J. P. *J. Organomet. Chem.* **1977**, *135*, 39.
(13) Cameron, C. J.; Wigley, D. E.; Wild, R. E.; Wood, T. E.; Walton, R. A. *J. Organomet. Chem.* **1983**, *255*, 345.
(14) Allison, J. D.; Wood, T. E.; Wild, R. E.; Walton, R. A. *Inorg. Chem.* **1982**, *21*, 3540.
(15) Cameron, C. J.; Tetrick, S. M.; Walton, R. A. *Organometallics* **1984**, *3*, 240.
(16) Barder, T. J.; Walton, R. A. *Inorg. Chem.* **1982**, *21*, 2510.
(17) Brignole, A. B.; Cotton, F. A. *Inorg. Synth.* **1972**, *13*, 85.

0020-1669/86/1325-3649$01.50/0 © 1986 American Chemical Society